This is a peer-reviewed, accepted author manuscript of the following article: Koubaiti, O., Fakkoussi, S. E., El-Mekkaoui, J., Moustabchir, H., Elkhalfi, A., & Pruncu, C. (Accepted/In press). Contribution to the treatment of constraints due to standard boundary conditions in the context of the mixed Web-spline finite element method. *Engineering Computations*.

Contribution to the treatment of constraints due to standard boundary conditions in the context of the mixed Web-spline finite element method

Ouadie Koubaiti[1], Said El Fakkoussi[1], Jaouad El-Mekkaoui[2], Hassan Moustabchir[3] Ahmed Elkhalfi[1], Catalin I. Pruncu[4,5]

[1] Faculty of Science and Technology of Errachidia, Department of Mathematics and Computer Science, Moulay Ismail University, Morocco

[2]Faculty Polydisciplinary of Beni-Mellal, Morroco

[3]Sidi Mohamed Ben Abdellah University, ENSA, Fez, Morocco

[4]Mechanical Engineering, Imperial College London, London, SW7 AZ, UK

[5] Design, Manufacturing & Engineering Management, University of Strathclyde, Glasgow, G1 1XJ, Scotland, UK.

Correspondence: Catalin.pruncu@strath.ac.uk ; c.pruncu@imperial.ac.uk , kouba108@gmail.com

Abstract:

This article proposes a new boundary condition using the web-spline that is formulated for a finite element space approximation. It enables to remedy the problems of constraints due to homogeneous and non-homogeneous Dirichlet boundary conditions.

The 2D linear Navier- Lamé elasticity equation with the condition $C_{A,B}$ is considered, which allows total insertion of the essential boundary conditions into the linear system obtained without the use of a numerical method such as the Lagrange multiplier. This development proposal of a mixed finite element method using B-splines Web-spline space offers an exact implementation of the homogeneous Dirichlet boundary conditions and eliminate the constraints imposed by the standard conditions. This offers proof of the existence and uniqueness of the weak solution, as well as convergence of the numerical solution for the quadratic case. The weighted extended B-spline approach is thus seen to offer a more practical solution.

Keywords: Inf-Sup condition, Navier-Lamé equation, $C_{A,B}$ generalized condition, Finite element, WEB-Spline, MATLAB.

1. Introduction

The mixed finite element method is a robust technique to solve difficult challenges from engineering and physical sciences using the partial differential equations. Some of the important applications include structural mechanics,

fluid flow, thermodynamics, and electromagnetic fields [2] that are mainly based on the approximation of Lagrange. However, this type of approximation has experienced a great restriction in the level of domain modelling, especially in the case of complicated boundaries such as that in the form of curvilinear graphs. There are some papers in literature which refer to mixed finite element method that enable to solve problem from several fields of physics, using the Gâteaux differential [30, 31, 32, 33, 34, 35] .

Recently, the research community tried to develop a new way of approximation based on the so-called B-spline that seems to have superior results in solving the engineering problems.

B-splines have become very important tools in approximation, computer graphics, design, and manufacturing. Recently, they have also been exploited to build basic functions for finite element methods. The resulting techniques combine the efficiency and simplicity of calculations on regular grids with the geometric flexibility of classical finite elements. Some key advantages are the freedom of choice of the order and the fluidity of calculations, this allows to obtain a simple data structure with one parameter per grid point and the exact representation of the boundary conditions. A type of B-spline is called (weighted extended B-splines) WEB-spline [11].

Researchers in the field of numerical methods have also developed a marked interest in meshless methods as a tool for solving problems with complex edges in science and engineering [24, 25, 26, 27, 36]. The main reason for this growing popularity is that these methods allow the use of trivial regular meshes where the elements of the mesh are uniform squares within an auxiliary domain of a simple form, often a square, into which the real domain is plunged, a formulation that allows the use of fast solvers for higher dimensions.

The main section of this report thus describes a situation in which a weighting function ω, is multiplied by the B-spline functions to adapt the WEB-splines exactly to the homogeneous and non-homogeneous Dirichlet boundary conditions, as these have not been checked for other classic functions. WEB-splines are a good choice for problems related to mixed boundary conditions with natural (Neumann) and essential boundary conditions (Dirichlet), as they have the advantage of applying practical implicit description of an edge for all types of edge using R-functions. A more comprehensive treatment of the relevant theory has been provided in existing works [4, 5].

Isogeometric methods borrow from the WEB-spline technique to manage domains that are parametrized on rectangles or cuboids or which can be expressed as the union or intersection of parametrizations of this type, such as the NURBS approach for CAD/CAM applications. Some problems can also be solved by combining the advantages of both techniques [6].

In this research, weighted finite element methods are implemented to solve the Navier-Lamé system with a new boundary condition $C_{A,B}$ [21], which generalises several well-known cases, especially the Dirichlet and the Neumann conditions. This novel proposed boundary condition permits the use of a single MATLAB code to summarise multiple boundary conditions encountered in the system. Using this model thus offers savings in terms of both processing time and programming resources as well as allowing the collation of several programs in a single directory.

The Navier equation contains only one unknown which is displacement. Further, in order to apply the method of the mixed finite element is required at least two unknowns. For that one creates another unknown which is

equal to the divergence of displacements, for instance. Besides, we have selected the application of a mixed method to prevent a large number of degrees of freedom, in turn it allowed us to have a good accuracy of the digital resolution.

The outline of this article is as follows: In the next section, the modelling of the Navier-Lamé equation is offered alongside the variational problem that corresponds to this equation, to permit a review of the preliminary aspects of applying WEB-spline-based methods for Navier-Lamé equations. In Section 3, the inf−sup conditions for the variational problem are then proved for the two-dimensional case using the WEB-spline-based mesh free method, as these are necessary allow the problem to be well-posed.

2. Navier-Lamé with novel boundary condition $C_{A,B}$

Linear elasticity as a mathematical study refers to how each point of a solid object may be displaced, producing a deformation, as the object becomes subjected to internal stresses due to the prescribed loading conditions. This is thus based on linear elasticity models of materials in a continuous state. Linear elasticity is a simple case of nonlinear elasticity theory and thus a branch of continuous domain mechanics. The basic theory of linear elasticity references the ideas that the strains (or stresses) involved are infinitesimal or small and that the relationships between the components of stress and strain are linear; in addition, linear elasticity is valid only for those states of stress which do not produce yield. These assumptions are reasonable for the analysis of many engineering materials and for use in technical design, and such analysis is often done using the finite element method.

If $\Omega \subset R2$ is a bounded Lipschitz domain with boundary condition Γ, which can be presented in a new form that generalises the Neumann and Dirichlet boundaries conditions, the Navier-Lamé equation governs all the assumptions previously noted about the linear relationship between strains and stresses. This section thus demonstrates the Navier-Lamé equation.

If a solid object is deformed under the action of forces applied, given $f \in L2(\Omega)$ and $A, B \in L\infty(\Gamma)2\times2$ are two invertible matrix functions, $g \in H1(\Gamma)$ and the positive parameters are λ and μ. A point in the solid, originally in (x, y), will move to (X, Y) at some point in time, and the vector $u = (u_1, u_2) = (X - x, Y - y)$ will represent the displacement. Where the movement is small and the solid is elastic, Hooke's law gives the relationship between the stress tensor and the strain tensor. Such that $\sigma = \lambda tr(\varepsilon)I2 + 2\mu\varepsilon$ is the stress tensor, $\varepsilon = 1/2\,(\nabla u + (\nabla u)^{\Gamma})$ is the strain tensor, I2 is the identity matrix, and μ is the shear modulus (or rigidity), where λ is Lam's first parameter. The Navier-Lamé equation is then given by the law of conservation of moment, $\rho a = div\sigma$, where a is the acceleration and ρ is the density of material. On the other hand:

$$div\sigma = \lambda div(tr(\varepsilon)I2) + 2\mu div\varepsilon \quad (1)$$

which gives:

$$div\sigma = \lambda div(tr(\varepsilon)I2) + \mu div(\nabla u) + \mu div(\nabla u)^{t} \quad (2)$$

Thus, applying a simple calculation, we found

$$div(tr(\varepsilon)I2) = div(\nabla u)^{t} = grad(div(u)) \quad (3)$$

Which further will generate

$$\rho a = \mu \Delta u + (\lambda + \mu)\mathrm{grad}(\mathrm{div} u) \quad (4)$$

If the solid is in dynamic equilibrium, $\rho a + f = 0$, where f refers to the external forces applied to the solid, finally, the equation becomes

$$f = -\mu \Delta u - (\lambda + \mu)\mathrm{grad}(\mathrm{div} u) \quad (5)$$

The work in [7, 8, 23, 22] offers more information on elasticity problems.

2.1 Novel boundary condition $C_{A,B}$

To present the new boundary condition $C_{A,B}$ several specific lemmas are required to facilitate subsequent calculations where mathematical boundary conditions have a matrix conception.

Lemma 1. *Either $n = (n_1, n_2)$ the normal vector on the edge of Ω faces outward. This allows assumption of the relationship*

$$n_1 \frac{\partial u_1}{\partial x} = -n_2 \frac{\partial u_2}{\partial x} \quad (6)$$
$$n_1 \frac{\partial u_1}{\partial y} = -n_2 \frac{\partial u_2}{\partial y}$$

The Neumann condition is then expressed in the form

$$\mu \frac{\partial u}{\partial n} + \lambda \nabla . un = g \quad (7)$$

Proof. According to Hooke's law the stress tensor is expressed as $\sigma = \lambda tr(\varepsilon) I2 + 2\mu\varepsilon$, which give

$$\sigma n = \lambda \mathrm{tr}(\varepsilon(u))n + 2\mu\varepsilon(u)n \quad (8)$$

This allows use of

$$\lambda \mathrm{tr}(\varepsilon(u))n = \lambda(\nabla . u)n \quad (9)$$

On the other hand,

$$2\varepsilon(u)n = \begin{pmatrix} 2n_1 \frac{\partial u_1}{\partial x} + n_2 \frac{\partial u_1}{\partial y} + n_2 \frac{\partial u_2}{\partial x} \\ 2n_2 \frac{\partial u_2}{\partial y} + n_1 \frac{\partial u_2}{\partial x} + n_1 \frac{\partial u_1}{\partial y} \end{pmatrix} = \begin{pmatrix} n_1 \frac{\partial u_1}{\partial x} + n_2 \frac{\partial u_1}{\partial y} \\ n_2 \frac{\partial u_2}{\partial y} + n_1 \frac{\partial u_2}{\partial x} \end{pmatrix} + \begin{pmatrix} n_1 \frac{\partial u_1}{\partial x} + n_2 \frac{\partial u_2}{\partial x} \\ n_2 \frac{\partial u_2}{\partial y} + n_1 \frac{\partial u_1}{\partial y} \end{pmatrix} \quad (10)$$

However, based on the relationship in (6),

$$\begin{pmatrix} n_1 \frac{\partial u_1}{\partial x} + n_2 \frac{\partial u_2}{\partial x} \\ n_2 \frac{\partial u_2}{\partial y} + n_1 \frac{\partial u_1}{\partial y} \end{pmatrix} = \begin{pmatrix} 0 \\ 0 \end{pmatrix} \quad (11)$$

Thus, simple calculation shows that it follows

$$\frac{\partial u}{\partial n} = \nabla u . n = \begin{pmatrix} n_1 \frac{\partial u_1}{\partial x} + n_2 \frac{\partial u_1}{\partial y} \\ n_2 \frac{\partial u_2}{\partial y} + n_1 \frac{\partial u_2}{\partial x} \end{pmatrix} \quad (12)$$

which offers a combination of (9), (11), (12), and (7). Throughout this work, the expression (9) is thus used to express the Neumann condition selected to simplify the calculations.

The essential boundary conditions (Dirichlet boundary conditions) usually create problems with constraints that offer difficulties in terms of the insertion of these constraints into variational problems (the penalty method, Lagrange

multipliers, etc.) at each step of the resolution. The difficulties produced by these constraints, at the level of the weak problem, the level of the approximate problem can be severe.

To remedy this, a new generalised condition, $C_{A,B}$, is implemented.

$$C_{A,B}: Au + B\left(\mu\frac{\partial u}{\partial n} + \lambda(\nabla.u)n\right) = g \text{ on } \partial\Omega = \Gamma \tag{13}$$

Where A and B are two invertible and bounded matrix functions belonging to $L\infty(\Gamma)$, with $\Gamma = \Gamma^D \cup \Gamma^N$, the matrices are of order 2 when working in 2D models, and of order 3 in the case of 3D models. These new boundary conditions have been constructed in order to generalise any standard type of boundary conditions (Dirichlet, Neumann, Robin, etc.). For example, the Dirichlet condition occurs when $|||B|||$ is negligible $|||A|||$, while the Neumann is usually not the only boundary condition in practical terms, thus requiring the addition of the Robin condition or a similar state, any of which are well presented by the new boundary condition $C_{A,B}$.

To illustrate the operation of this boundary condition, the following example can be used. Consider a rectangular domain with $\Gamma = U^4$ and Γi as its edge. By setting $\Gamma^D = \Gamma_3$ and $\Gamma^N = \Gamma_1 \cup \Gamma_2 \cup \Gamma_4$, the following boundary conditions are considered:

$$\begin{cases} u = (a(x,y),(b(x,y)), on\ \Gamma_3 \\ \mu\frac{\partial u}{\partial n} + \lambda\nabla.un = (c(x,y),(d(x,y)), on\ \Gamma_1 \\ \mu\frac{\partial u}{\partial n} + \lambda\nabla.un = 0\ , on\ \Gamma_2 \\ \mu\frac{\partial u}{\partial n} + \lambda\nabla.un = 0\ , on\ \Gamma_4 \end{cases} \tag{14}$$

Assuming that functions a, b, c, and d are non-zero and bounded on Γ, the system (14) can then be expressed as the boundary condition

$$C_{A,B}: Au + B\left(\mu\frac{\partial u}{\partial n} + \lambda(\nabla.u)n\right) = g \text{ on } \partial\Omega = \Gamma$$

Setting displacement u to Ω then allows the matrix notation of the $C_{A,B}$ boundary condition to be written as

$$\begin{pmatrix} \frac{1}{a(x,y)} & 0 \\ 0 & \frac{1}{b(x,y)} \end{pmatrix}\begin{pmatrix} u_1|_{\Gamma_D} \\ u_2|_{\Gamma_D} \end{pmatrix} + \begin{pmatrix} \frac{1}{c(x,y)} & 0 \\ 0 & \frac{1}{d(x,y)} \end{pmatrix}\begin{pmatrix} \mu\frac{\partial u_1}{\partial n}|_{\Gamma_N} + \lambda(\nabla.u|_{\Gamma_N})n_1 \\ \mu\frac{\partial u_2}{\partial n}|_{\Gamma_N} + \lambda(\nabla.u|_{\Gamma_N})n_2 \end{pmatrix} = \begin{pmatrix} \xi_1(x,y) + \xi_3(x,y) \\ \xi_1(x,y) + \xi_3(x,y) \end{pmatrix} \tag{15}$$

For $i = 1$ or 3, the following functions are defined:

$$\xi_i(x,y) = \begin{cases} 1 & if\ (x,y) \in \Gamma_i \\ 0 & if\ not\ (x,y) \notin \Gamma_i \end{cases} \tag{16}$$

According to the system (15) will enable

$$A = \begin{pmatrix} \frac{1}{a(x,y)} & 0 \\ 0 & \frac{1}{b(x,y)} \end{pmatrix}, B = \begin{pmatrix} \frac{1}{c(x,y)} & 0 \\ 0 & \frac{1}{d(x,y)} \end{pmatrix} \tag{17}$$

A new unknown, the relative increase of volume due to deformation (dilatation) $\psi = \nabla.u = \frac{\partial u_1}{\partial x} + \frac{\partial u_2}{\partial y}$ that is equal to divergence of the displacement is set, and the Navier- Lamé equation thus becomes

$$\begin{cases} -\mu\Delta u - (\lambda+\mu)\nabla\psi & = f \ in\ \Omega \\ \psi - \nabla.u & = 0 \ in\ \Omega \\ Au + B\left(\mu\frac{\partial u}{\partial n} + \lambda(\nabla.u)n\right) & = g \ on\ \Gamma \end{cases} \quad (18)$$

This mathematical model is a Navier- Lamé system with a new boundary condition, $C_{A,B}$ such that A is a Dirichlet matrix and B is a Neumann matrix. There are two strictly positive constants α and β, such that

$$\alpha u.u \ \leq \ \mathrm{B}^{-1}\mathrm{Au.u} \ \leq \ \beta \mathrm{u.u}\ \forall \mathrm{u} \ \in \ \mathrm{R}^2 \quad (19)$$

where $|||\ .\ |||$ is a matrix norm, as defined below.

Thus, if $|||\ \mathrm{A}\ ||| \ll |||\ \mathrm{B}\ |||$, then $C_{A,B}$ is the Neumann boundary and if

$|||\ \mathrm{B}\ ||| \ll |||\ \mathrm{A}\ |||$ then $C_{A,B}$ is the Dirichlet boundary.

2.2 Weak problem of Navier-Lamé with new boundary condition $C_{A,B}$

Functional spaces and norms must be defined initially.

$$h1(\Omega) \ = \ \{u: \ \Omega \ \rightarrow \ R \setminus u, \frac{\partial u}{\partial x}, \frac{\partial u}{\partial y} \ \in \ L2(\Omega)\}, \quad (20)$$

$$V\ (\Omega) \ = \ H1(\Omega) \ = \ [h1(\Omega)]2 \quad (21)$$

$$M\ (\Omega) \ = \ L2(\Omega) \ = \ \{q \ \in \ L2(\Omega) \setminus \int_\Omega \ q = 0 \quad (22)$$

$$||\ v||_{1,\Omega} = \left\{\int_\Omega \ \nabla v : \nabla v d\Omega + \int_\Omega \ v v d\Omega\right\}^{1/2} \quad (23)$$

$$||\ v||_{0,\Omega} = \left\{\int_\Omega \ v v d\Omega\right\}^{1/2} \quad (24)$$

$$\left|\left||A|\right|\right| = max\left|a_{i,j}\right| \ i = 1.2, j = 1.2 \quad (25)$$

The variational formulation of the Navier-Lamé problem (18) is as follows:

Determine $(\mathrm{u}, \psi) \ \in \ \mathrm{V}\ (\Omega) \ \times \ \mathrm{M}\ (\Omega)$ such that

$$\begin{cases} \int_\Omega \ \mu\nabla\mathrm{u} : \nabla\mathrm{v}d\Omega + \int_\Gamma \ \mathrm{B}^{-1}\ \mathrm{Au.v}d\Gamma \\ -\int_\Gamma \ \mathrm{u}\psi\mathrm{n.v}d\Gamma + \int_\Omega \ (\lambda+\mu)\psi\nabla.\mathrm{v}d\Omega \\ \quad = \int_\Omega \ \mathrm{f,v}d\Omega + \int_\Gamma \ \mathrm{B}^{-1}\ \mathrm{g.v}d\Gamma \\ \int_\Omega \ (\lambda+\mu)\mathrm{q}\nabla.\mathrm{u}d\Omega - \int_\Omega \ (\lambda+\mu)\psi\mathrm{q}d\Omega = 0 \end{cases} \quad (26)$$

The weak formulation (26) may be restated as:

Find $(\mathrm{u}, \psi) \ \in \ \mathrm{V}\ (\Omega) \ \times \ \mathrm{M}\ (\Omega)$

$$\begin{cases} a(u,v) \ + \ b_\Gamma \ (v,\psi) \ = \ L(v)\ \forall v \ \in \ V\ (\Omega) \\ \ b(u,q) \ - \ d(\psi,q) \ = \ 0\ \forall q \ \in \ M\ (\Omega) \end{cases} \quad (27)$$

With bilinear forms as:

$$\begin{cases} a(u,v) = \int_\Omega \mu \nabla u : \nabla v d\Omega + \int_\Gamma B^{-1} Au.vd\Gamma \\ b(v,q) = \int_\Omega (\lambda+\mu) \mathrm{q}\nabla.vd\Omega \\ b_\Gamma(v,q) = b(v,q) - \int_\Gamma \mu qn.vd\Gamma \\ d(\psi,q) = \int_\Omega (\lambda+\mu)\psi \mathrm{q} d\Omega \\ L(v) = \int_\Omega f,vd\Omega + \int_\Gamma B^{-1} g.vd\Gamma \end{cases} \quad (28)$$

This allows total insertion of the conditions at the limits in the weak formulation of the problem, which allows a smoothing of the numerical calculations later in the context of the numerical resolution of the problem.

The well-posed nature [1, 9, 10] of this formulation is demonstrated as follows: For variational problem (27), the mapping:

$$Ł : V(\Omega) \times M(\Omega) \longrightarrow X^* \times M^* \quad (29)$$

defines an isomorphism if and only if a, b, b_Γ, and d satisfy assumptions (30) ... (35).

Within the ensuing spaces, V*, M* are respectively the topological duals of the functional spaces V(Ω) and M(Ω), which are in turn respectively defined by the formulas (21) and (22).

$$\begin{aligned} &| \mathrm{b_1(u,q)} | \leq \|\mathrm{b_1}\| \, \|\mathrm{u}\|_{1,\Omega} \|\mathrm{q}\|_{0,\Omega} \forall (\mathrm{u,q}) \in \mathrm{V_0}(\Omega) \times \mathrm{M_0}(\Omega) \\ &| \mathrm{b_2(u,q)} | \leq \|\mathrm{b_2}\| \, \|\mathrm{u}\|_{1,\Omega} \|\mathrm{q}\|_{0,\Omega} \forall (\mathrm{u,q}) \in \mathrm{V_0}(\Omega) \times \mathrm{M_0}(\Omega) \\ &| \mathrm{d(q,p)} | \leq \|\mathrm{d}\| \, \|\mathrm{q}\|_{0,\Omega} \|\mathrm{p}\|_{0,\Omega} \forall (\mathrm{p,q}) \in \mathrm{M_0}(\Omega) \times \mathrm{M_0}(\Omega) \\ &| L(v) | \leq \|L\| \, \|v\|_{1,\Omega} \forall v \in V_0(\Omega) \\ &| G(q) | \leq \|G\| \, \|q\|_{0,\Omega} \forall q \in M_0(\Omega) \end{aligned} \quad (30)$$

The following Hilbert spaces are also defined:

$$B_i = \{u \in V_0(\Omega) \backslash b_i(u,q) = 0 \, \forall q \in M_0(\Omega)\}, for \; i = 1,2 \quad (31)$$

$$D = \{p \in M_0(\Omega) \backslash d(p,q) = 0 \forall q \in M_0(\Omega)\} \quad (32)$$

In addition to assumption (30), it is also assumed that

$$a(v,v) \geq \delta \, \|v\|^2_{1,\Omega} \; for \; all \; v \in V_0(\Omega) \quad (33)$$

b_i, for $i = 1, 2$ satisfies the inf−sup condition such that there exists a constant $\varrho > 0$

$$sup_{||q||=1} b_i(v,q) \geq \varrho_i ||v||_{1,\Omega} \forall v \in B_i^\perp \quad (34)$$

$$sup_{v \epsilon B_i^\perp} bi(v,q) > 0 \, \forall q \in M0(\Omega)$$

and that the bilinear form d satisfies the condition of weak coerciveness, as there exists a constant $\varepsilon > 0$ such that

$$\mathrm{Sup}_{q \epsilon M_{0(\Omega)}} d(p,q) \geq \varepsilon \, \|p\|^2_{0,\Omega} \forall p \in M_0(\Omega) \quad (35)$$

3. WEB-Spline process

B-splines are fundamental in almost all geometric modelling applications. Non-uniform rational B-spline representations (Nurbs) (Bazilevs et al. 2008, [22]) have become standard in CAD and CAM (Shah et al. 1995, [23]) work, and by applying the WEB method, B-splines have also been found to provide highly efficient finite element

approximations. The B-splines located near the edge of a domain offer very little relevant support and thus cause instabilities in the numerical solution; however, they cannot be omitted without affecting the order of approximation and producing a large number of conditions within the resulting linear system. The main remedy for this numerical instability is to join the external B-splines to the internal B-splines by forming appropriate linear combinations.

To obtain a high-quality finite element approximation, the correct choice of coefficients for the required combination is necessary. By joining the external and internal B-splines, a new category of B-splines called extended B-splines is created, which are endowed with stability. They thus form a stable base with all the characteristic properties of finite elements. As stability is only necessary locally, near the edge B-splines, areas inside the domain are not modified. In particular, for small gate widths, the majority of internal B-splines remain unchanged.

Building the WEB base is simple: the relevant B-splines are classified into internal and external B-splines, depending on the size of their support in the simulation region. To stabilise the base, the external B-splines are then joined to the internal B-splines by creating appropriate linear combinations. This is a crucial step, and the coupling coefficients are chosen so as to maintain local support and the approximation power of the selected B-splines. In addition, optional weighting of the basic functions allows for more exact fulfilment of essential boundary conditions. Several types of non-mesh approaches have been proposed for this within various applications. A major problem with the Galerkin method without mesh is the requirement to insert homogeneous and nonhomogeneous Dirichlet boundary conditions, yet the extended weighted B-spline approximation not only manages the constraints arising from Dirichlet's boundary conditions but also addresses the question of good conditioning for Galerkin systems [11].

Identifying the essential new characteristic for construction of a stable and suitable base using the part of the edge which presents the embedding (Dirichlet) is of capital importance in this work. The aim is to apply the approximation properties of the spaces generated by the web-splines to discretise the Navier-Lamé equations as has previously been done for the Stokes and Navier-Stokes [13] problems.

The standard uniform B-spline of degree n is defined by the recursion [5]

$$B^n(x) = \frac{x}{n}B^{n-1}(x) + \frac{n+1-x}{n}B^{n-1}(x-1) \tag{36}$$

starting from B^0, with the characteristic function of the unit interval between zero and one. Figures 1, 2, and 3 show uniform B-splines of one, two, and three degrees, also known as linear, quadratic, and cubic B-splines, respectively. The following notational conventions [5] are used to clarify the ensuing work. For functions f and g, we write:

$$f \leq g \Longleftrightarrow f \leq cg \tag{37}$$

For $k = (k_0, k_1) \in Z^2$ where $h > 0$, a B-spline in 2D is defined as

$$B_k(x,y) \coloneqq \frac{1}{h}B\left(\frac{x}{h} - k_0\right)B\left(\frac{y}{h} - k_1\right) \tag{38}$$

B is the univariate B-spline of degree n with support [0, n + 1), and the B-splines B_k are polynomials on the h-grid with vertices $h\mathbb{Z}^2$ scaled such that the L^2-standard, $||Bk|| = ||B0||_{0,\Omega}$ is independent of h.

The tensor product B-spline is the extension of B-spline to higher dimensions; in general, it can be defined as

$$B_{k,h}^{n} = II_{v=1}^{m} B_{k_{v,h}}^{n_v} \tag{39}$$

Such that the B-spline $B_{k,h}^{n}$ is an m-variant of degree n_v in the v^{th} variable, index $k = k1, \ldots, km$, and the width of the grid is h.

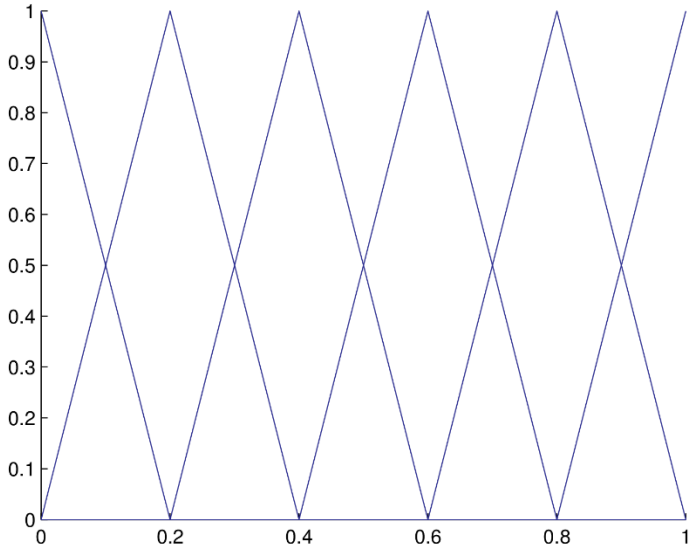

Figure 1: Linear B-Spline

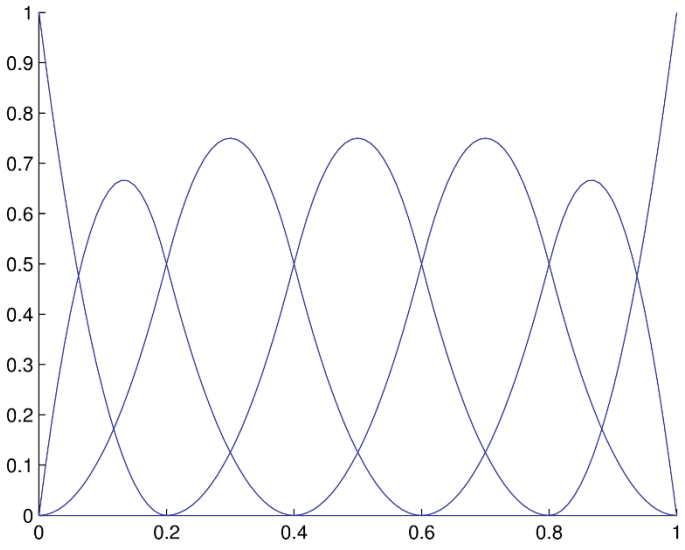

Figure 2: Quadratic B-Spline

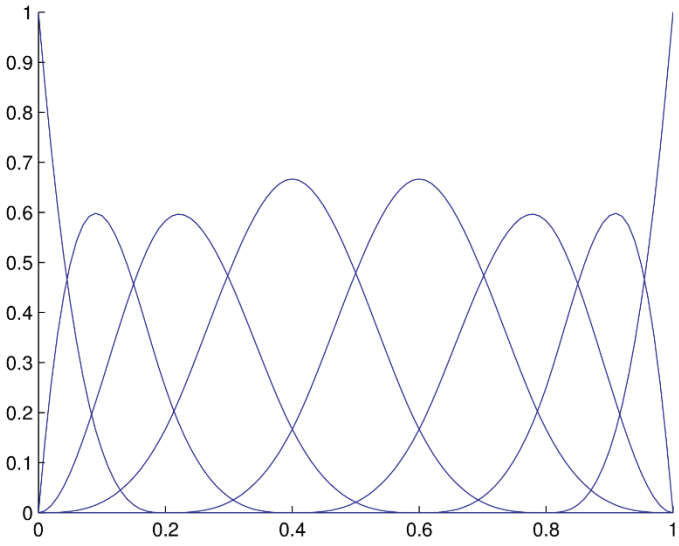

Figure 3: Cubic B-Spline

Using the convention that $n_1 = \ldots = n_m$, unless otherwise indicated, for the sake of the problem, the element n can be taken as an integer, rather than an integer vector.

For $I \in \{0, \ldots, n\}^m$, the cells of the grid are thus distributed as follows:

$$Q_I = Ih + [0,1]^m h \tag{40}$$

$m = 2$ in the case of 2D, and there are three types of Q cell:

- interior cells: $Q \subset \overline{\Omega}$,
- cells at the edge, where the inside of Q cuts $\partial\Omega$,
- outside cells: $Q \cap \Omega = \emptyset$.

The support for the B-spline B_k of order n in two dimensions is

$$supp\, B_k = hk + [0, nh]^2, k \in \mathbb{Z}^2 \tag{41}$$

For $k \in K := \{I \in Z^2 : supp(B_I) \cap \Omega \neq \emptyset\}$ (the relevant index defined for Ω). If $supp(B_k)$ has at least one grid cell completely inside Ω, then B_k is an internal B-spline; otherwise, it is external. The corresponding subsets of K are I and J such that: $K = I \cup J$ (see Figure 4). More details on the construction of the Web-Spline database are given by Höllig et al. in [5].

While it may seem tempting to use $Bh := span\{Bk : k \in K\}$ as a finite element approximation space, this does not seem feasible initially, as the function Bk does not conform to the boundary conditions. This difficulty can be easily resolved by multiplying Bk by a smoothed distance function, however:

$$\omega(x) \sim dist(x, \partial\Omega) \tag{42}$$

Then, the weighted space B-spline (WB-space) becomes

$$B_\omega^h := span\{\omega B_k : k \in K\} \tag{43}$$

which is generated by weighted B-splines to create a possible finite element subspace for Dirichlet problems based

on optimal order approximations.

Nevertheless, the condition number of the Galerkin matrix G_h can become extremely large in this manner due to external B-splines having only a small part of their support inside Ω.

As this type of basic function does not contribute much to the approximation power, some researchers might assume it can simply be omitted. Unfortunately, this is not the case. However, an appropriate solution to the problem of controlling unstable external B-splines is provided by properly joining them to internal B-splines to preserve the power of approximation of the finite element subspace.

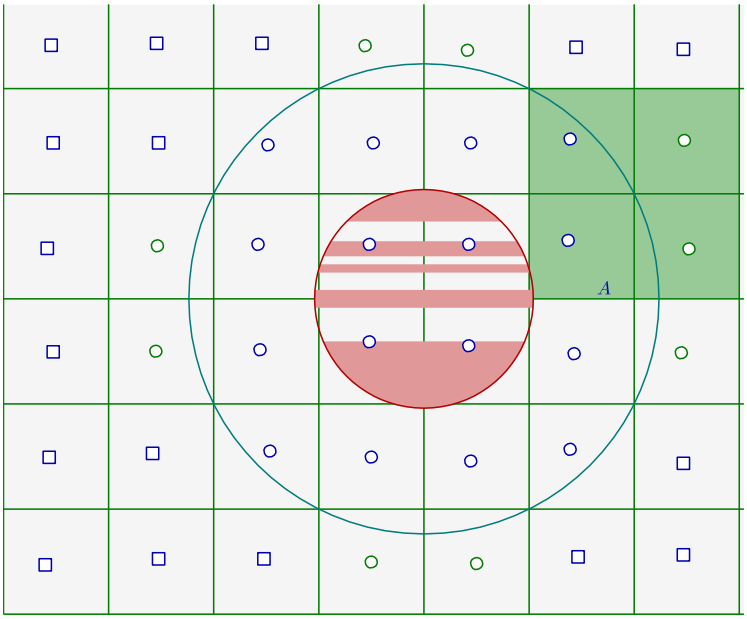

Figure 4: Quadratic B-splines relevant to domain A, marked in the center of their internal B-spline supports with circles and the external ones with squares.

Lemma 2. For $i \in I$, the Web-spline basis B_i is defined by

$$B_i = \frac{\omega}{\omega(x_i)}\left[b_i + \sum_{j\in J} e_{i,j} b_j\right] \tag{44}$$

where x_i indicates the centre of a grid cell that is entirely located in the domain Ω.

The coefficients $e_{i,j}$, satisfy $|e_{i,j}| \leqslant 1$, $e_{i,j} = 0$ for $||\, i - j|| \geqslant 1$ and are chosen so that all weighted polynomials (ωp) of order n are contained within the spline web space:

$$B_h := span\{B_i : i \in I\} \tag{45}$$

(see K. Höllig et al. 2001, [11])

Remark 1. *The external B-splines are retained purely for reasons that have nothing to do with finite elements.*

Indeed,

$$\sum_{j=1}^{N}\sum_{k=1}^{N} c_{j,k}b_{j,k} \quad (46)$$

with coefficients $c_{j,k}$ equal to 0, is easier to use than

$$\sum_{i=1}^{M} c_{j(i),k(i)}b_{j(i),k(i)} \quad (47)$$

This produces a simple data structure, a rectangular index table, without the need for connectivity lists (see Höllig et al. 2015, [15, 16, 17]).

The theory underlying the use of $e_{i,j}$ is complicated. Fortunately, to achieve an optimal order of convergence, it is not necessary; it is only necessary to prove the stability of the B-spline base. Thus, it is possible to work with all the B-splines that overlap the domain without modification.

The square 4 is only the set used to define the base B-spline, with the field of FEM simulation being the curved set inside such a square. The B-splines are limited to this set in that only the part that overlaps the curved set is used.

Theorem 3. For an external index $j \in J$, let $I(j) = l + \{0,\dots,n\}m \subset I$, a dimensional array m of internal indices closest to j is assumed to exist wherever h is small enough for such an array to exist. This means that the coefficients:

$$e_{i,j} = \prod_{v=1}^{m}\prod_{\mu=0}^{n}\prod_{\iota_{v+\mu}\neq i_v}\frac{j_v-\iota_v-\mu}{i_v-\iota_v-\mu} \quad (48)$$

are eligible for the construction of WEB-Splines according to definition 2. (see Höllig et al.2001, [11]).

4. $C_{A,B}$ boundary conditions with adapted resolution

The imposition of inhomogeneous Dirichlet boundary conditions is essential in numerical analysis of a structure; however, this is not straightforward where non-conformal mesh is used to discretise a structure. One of the contributions of this paper is thus to develop a weighted extended spline basis with high computing accuracy appropriate for use with the new mixed formulation of boundary conditions, $C_{A,B}$, that generalises all the cases that may be encountered on the edge of Ω.

$$Au + B\left(\mu\frac{\partial u}{\partial n} + \lambda\nabla.un\right) = g \; on \; \Gamma \quad (49)$$

where A and B are two reversible square (in the case of 2D models) matrices. $A, B \in L^{\infty}(\Gamma)^{2\times 2}$ and $g \in H^{1/2}(\Gamma)$ where the function g is an a priori known function of spatial coordinates. The inhomogeneous Dirichlet condition is expressed in the case of B = 0, to obtain $u = A^{-1}g$ on Γ. In general, a boundary condition function g may not be known explicitly or may not be prescribed globally; more typically, the boundary conditions are prescribed in a piecewise manner such that boundary conditions are specified by individual functions g_i on each portion of boundary, $u = A^{-1}g_i \; on \; \Gamma_i$

such that $i = 1, \dots N$ and $\Gamma_i \cap {}_i\Gamma_i = \emptyset$. If each Dirichlet boundary Γi is geometrically represented as $\Gamma = \cup_{i=1}^{N}$; the implicit nature of function ω_i means that $\omega_i = 0$ on Γ_i, [19]

$$u = A^{-1}gi\,, \forall \omega i = 0 \tag{50}$$

As the weighting function and boundary value function are expressed in the form of implicit functions, no unique expressions exist; however, typical forms are given below.

The weighting function $\omega(x)$ acts as a multiplier that modifies the original interpolation functions and thus disappears on any Dirichlet boundary ($\omega_i(x) = 0$). As implicit functions are not unique for this definition, weighting functions of different forms can be used, as discussed in [18]. Here, two construction techniques are presented.

The first, a relatively straightforward method, constructs the weighting function by means of the product $\omega(x) = \prod_{i=1}^{m} \omega_i(x)$. Clearly, $\omega(x) = 0$ if any $\omega_i(x) = 0$ on Γ_i. Nevertheless, a product of all implicit functions might lead to a surge of function values, causing a numerical overflow and resulting in poor computing accuracy and robustness. Each implicit function ω_i should thus be normalised in advance based on the size of the physical domain. For instance, the implicit function of a circle can be normalised in terms of its radius.

$$\omega(x) = 1 - \left(\frac{x-x_0}{R}\right)^2 - \left(\frac{y-y_0}{R}\right)^2 \tag{51}$$

Web-spline basis functions must then be adopted. The basis these form will respond to any type of non-homogeneous boundary conditions, especially $C_{A,B}$ in the case where $B = 0$. Let u be the displacement solution of the problem (27), to give $u = u_0 + u_\Gamma$, with u_0 as the solution of (27) in the case of a homogeneous Dirichlet boundary and $u_\Gamma = A^{-1}g$ where there is a nonhomogeneous Dirichlet boundary. Here, u is written as a linear combination of the B_i web-spline family cited in definition (2)

$$u = \sum_{i=1}^{N} u_i B_i + A^{-1}g \tag{52}$$

This can thus be rewritten in the form

$$\mathrm{u} = \sum_{\mathrm{i}=1}^{\mathrm{N}} \mathrm{u_i B_i} + \sum_{\mathrm{i}=1}^{\mathrm{N}} \mathrm{b_i A^{-1} g_i} \tag{53}$$

where $b_i(x)$ denotes the i^{th} weighting coefficient associated with $A^{-1}g_i$, where the basic properties of $b_i(x)$ are [19] that $b_i = \delta ij\,, i,j = 1, 2...N$, with δij denoting the Kronecker delta function.

Under this condition, several different forms can be used for the definition of b_i.

In transfinite interpolation form, the weighting coefficients are defined by extending the transfinite interpolation developed by Rvachev et al. [20] in the CAD community.

$$\mathrm{b_i} = \frac{\prod_{\mathrm{j=1,i\neq j}}^{\mathrm{N}} \omega_{\mathrm{j}}^{\theta}}{\sum_{\mathrm{k=1}}^{\mathrm{N}} \mathrm{j=1,i\neq j}} \tag{54}$$

This equation holds the properties of symmetry and similarity, and $\omega_j(x)$ is generally held to be positive in the physical domain to ensure a non-zero value of the denominator. Evidently, $b_i = 1$, only if $\omega_i = 0$, and the partition of unity holds with $\sum_{i=1}^{N} b_i = 1$. The value of θ, used to interpolate normal derivatives prescribed on Γ, must therefore be one greater than the order of the prescribed derivatives. This means that basis proposed for the non-

homogenous boundary condition is :

$$\{\varphi i\}i = 1,..N \quad = \{Bi \ + \ bi\}i = 1,..N \tag{55}$$

5. Discretization of the Navier-Lamé problem Using WEB-Spline Basis

In the Navier-Lamé problem, Δu and $\nabla\psi$ are the terms with derivatives of highest order for the displacement and dilatation (ψ), respectively. Thus, the orders of the differential operators differ by 1, which suggests a rule of thumb that the degree of the basic functions used to approximate the displacement should be one larger than that used for the approximation of the dilatation. To satisfy the Dirichlet boundary conditions, the displacement basis functions must also be multiplied by a suitable weight function, ω. This work uses a φ_j -linear weighted extended B-spline for displacement approximation along with a ϕ_i-Haar wavelet basis function for dilatation approximation as the linear-constant element; for the quadratic-linear element, φ_j is used as the quadratic WEB-spline and ϕ_i as the mean zero linear function (see Figures 1 and 2), as defined above. In the following section, the inf−sup condition is settled first for the linear-constant element and then for the quadratic-linear element, indicating that the discrete Navier-Lamé problem is well-posed.

Linear constant element: More precisely, V_h and M_h, the displacement and dilatation finite element spaces respectively can be defined as follows:

$$V_h = \{(u_1, u_2)/u_k = \sum_{j=\epsilon I^u} \alpha_j^k \phi_j, \alpha_j^k \in \mathbb{R}, k = 1,2\} \tag{56}$$

$$M_h = \{\psi/\psi = \sum_{j=\epsilon I^\psi} \beta_i^k \varphi_j, \beta_i \in \mathbb{R}\} \tag{57}$$

A sufficient condition for (V_h, M_h) to satisfy the inf−sup condition is given in [13], and a similar result was proved in [14] for a different pair (V_h, M_h).

Quadratic-linear element for $j \in I^\psi$

$$\varphi_j(x,y) = \frac{1}{h}\varphi(\frac{x}{h} - j_0)\varphi(\frac{y}{h} - j_1) \tag{58}$$

where φ is as defined below:

$$\varphi(x) := \begin{cases} x \ on \ [0,1) \\ 2 - x \ on \ [1,2) \\ 2 - x \ on \ [2,3) \\ x - 4 \ on \ [3,4) \end{cases} \tag{59}$$

To construct the displacement approximation space, the following steps are required: For $i \in I^u$, let φ_i be a WEB-spline of order 3, as given by (44) and (55) where φ_i is defined as in (58) as the tensor product of the scaled translation of the function φ,

$$\varphi(x) := \begin{cases} \frac{x^2}{2} \; on \; [0,1) \\ \frac{1}{2} + (x-1) - (x-1)^2 \; on \; [1,2) \\ \frac{(3-x)^2}{2} \; on \; [2,3) \end{cases} \tag{60}$$

$$V_b \coloneqq \oplus k \epsilon T_h \, V_K \tag{61}$$

where the quadrangulation T_h is the collection of all cells $K \subset \Omega$ such that $K \cap \partial\Omega = \emptyset$ (those which are fully inside the domain Ω) and $K_{\partial\Omega} := K \cap \Omega \neq \emptyset$ such that $K \cap \partial\Omega \neq \emptyset$ (those portions which intersect the boundary $\partial\Omega$) and V_K is the one dimensional subspace spanned by the function b^K, given by

$$b^K \coloneqq \omega(x,y) b\left(\frac{x}{h} - k_0\right)\left(\frac{y}{h} - k_1\right) \tag{62}$$

The function $b(x) := x(x-1)$ is then chosen so that the bubble function b^K vanishes on the edges of cell K. The node corresponding to cell K is (k_0, k_1), and the weight function w is multiplied to ensure that bubble function also vanishes on the boundary $\partial\Omega$. The distance function is used near the boundary, where it is free of singularities and blends smoothly with a plateau inside the domain.

More precisely, ω is defined as: $\omega = 1 - \left(\left(\frac{\max(\delta - d(x), 0)}{\delta}\right)^l d(x) = dist(x, \partial\Omega)\right.$, where δ controls the height of the plateau and l represents the smoothness of the weight function. The plateau facilitates the use of precomputed values during assembly of the Galerkin matrix and also avoids the use of high-order quadratures for the integration of the bubble functions supported on those cells which are fully inside the domain.

The displacement approximation space is thus taken to be. $V_h^2 := V_h \oplus V_b$

The pair (V_h^2, M_h) of discretization spaces thus satisfies the discrete inf−sup condition.

Lemma 4. *A web- basis* $\{B_i\}_{i\in I}$ *is a stable basis with respect to* L^2*-norm,* $C_1||\{a_i\}_{i\in I}|| \leq ||\sum_{i\in I} B_I||_0 \leq C_2||\{a_i\}_{i\in I}||$*, where* C_1, C_1 *are constants.([11]).*

We can also bound higher order Sobolev norms in terms of the 2-norms of the coefficients.

Lemma 5. *A web- basis* $\{B_i\}_{i\in I}$ *satisfies*

$\|\sum_{i\in I} a_i B_i\|_1 \leq |C_3 h^{-1}| \|\{a_i\}_{i\in I}\|$*, and* $C3 > 0$ *is a constant.([11]).*

Lemma 6. *(Inverse estimate)*

Let V_h be the finite element space considered as in (56). There thus exists a constant C such that

$\|\sum_{i\in I} a_i B_i\|_1 \leq C_6 h^{-1} \|\sum_{i\in I} a_i B_i\|_0$.

The proof of this follows from Lemmas 4 and 5.

Lemma 7. *Suppose* T_h *is a family of uniform quadrilateral meshes on the domain* Ω *and* $\prod_h$ *is the L2-projection*

operator onto $V_h \subset H^1(\Omega)$. *Then*

$$\|\prod_h v\|_1 \leq C \|v\|_1, \forall v \in H_0^1(\Omega) \quad (63)$$

where C is a constant which is h-independent ([13]).

Lemma 8. *There exists an operator* $P_h: H^1(\Omega) \rightarrow V_h^2$ *which satisfies the following properties:*

$$b(P_h v, q_h) = b(v, q_h), \forall q_h \in M_h \quad (64)$$

$$b_\Gamma(P_h v, q_h) = b_\Gamma(v, q_h), \forall q_h \in M_h \quad (65)$$

$$\|Phv\|_1 \leq C \|v\|_1, C > 0 \text{ independent of } h \quad (66)$$

Proof. Let $P^0: H_h^1(\Omega) \longrightarrow V_h$ be the usual L^2- projection operator with:

$$\left\|P_h{}^0 v\right\|_1 \leq c_1 \|v\|_1 \quad (67)$$

$$\left\|v - P_h{}^0 v\right\|_0 \leq c_2 h \|v\|_1 \quad (68)$$

The first inequality (67) follows from lemma (7) and the density of $H_0^1(\Omega)$ in $H^1(\Omega)$ $\left(\overline{\left(H_0^1(\Omega) \cap V\right)}^{\|.\|_{1,\Omega}} \subset H^1(\Omega)\right)$, while the second (70) is an L2− error estimate.

A linear mapping $P1 : L2(\Omega) \xrightarrow[h]{} Vb$ is then fixed such that:

$$\int_k P_h^1 v = \int_k v, for\ each\ K \in T_h \quad (69)$$

The map P_h^1 can be interpreted as a process with two steps. The $L2-$ projection is first applied to the space of the piecewise constant functions; then, in each cell, the constant K is replaced by a bubble function with the same integral. This gives:

$$\left\|P_h{}^1 v\right\|_0 \leq c_3 \|v\|_0 \quad (70)$$

P_h^1 is thus defined as follows:

$$P_h^1 v_{|K}(x, y) = \beta(K) b^K(x, y), \text{ for each } K \in \mathrm{T}_h \quad (71)$$

In view of condition (69), the constant β(K) is taken to be $\frac{\int_k v}{\int_k b^K}$.

This means that $\int_k b^K = c_4 h^2$ and $\int_k (b^K)^2 = c_5 h^2$, where c4, c5 > 0 are constants.

$$\|P_h^1 v\|_0^2 = \sum_{K \in T_h} \int_k |P_h^1 v|^2 = \sum_{K \in T_h} \int_k \beta(K)^2 (b^K)^2 \quad (72)$$

$$= \sum_{K \in T_h} \frac{\int_k v}{\int_k b^K} \int_k (b^K)^2 \quad (73)$$

$$\leq \frac{1}{(c_4)^2 h^4} \sum_{K \in T_h} \left(\int_k v^2\right) |K| c_5 h^2 \quad (74)$$

$$= \left(\frac{c_5}{(c_4)^2}\right) \|v\|_0^2 \quad (75)$$

The above inequality occurs due to Cauchy-Schwartz and $| K | = h^2$ with reference to the area of the cell *K*. Setting

$$P_h v = P_h^0 v + P_h^1 (v - P_h^0 v) \tag{76}$$

thus, verifies the two properties in the statement of the lemma by the virtue of the construction of P^h. The term $v - P_h^0 v = 0$ can then be imposed on $\partial\Omega$.

$$\int_K (v - P_h v) = \left| \int_K (I - P_h^1)(v - P_h^0 v) = 0 \; \forall K \in T_h \right. \tag{77}$$

Because q_h is piecewise linear, Green's theorem can be applied,

$$b(v - P_v v, q_h) = \int_\Omega div(v - P_v v) q_h \tag{78}$$

$$= \int_{\partial\Omega} (v - P_v v) q_h - \int_\Omega (v - P_v v) \nabla q_h \tag{79}$$

$$= - \sum_{K \in T_h} C_K \int_\Omega (v - P_v v) = 0 \tag{80}$$

and it is easy to prove (65) by applying Green's theorem and using (64):

$$\| P_h v \|_1 \leq \left\| P_h{}^0 v \right\|_1 + \| P_h^1 (v - P_h^0 v) \|_1 \tag{81}$$

$$\leq c_1 \| v \|_1 + c_6 h^{-1} \| P_h^1 (v - P_h^0 v) \|_0 \tag{82}$$

$$\leq c_1 \| v \|_1 + c_6 h^{-1} c_3 \| (v - P_h^0 v) \|_0 \tag{83}$$

$$\leq c_1 \| v \|_1 + c_6 h^{-1} c_3 c_2 h \| v \|_1 \tag{84}$$

$$\leq c \| v \|_1 \tag{85}$$

This proves assertion (66) with $c = c_1 + c_6 c_3 c_2$, such as the c_6 of lemma (6).

Theorem 9. *Let consider the space*

$$Bh = \{ u \in H^1(\Omega) \backslash b(Phu, qh) = 0 \, , \forall qh \in Mh(\Omega) \} \tag{86}$$

such as $V_h^2 = Bh \oplus Bh^\perp$. The pair (V_h^2, M_h) thus satisfies the discrete inf − sup condition:

$$\exists \lambda_0 > 0, sup_{||q_h||_0 = 1} \frac{b(v_h, q_h)}{||v_h|| V_h^2} \geq \lambda_0, \forall v_h \in Bh^\perp \tag{87}$$

$$sup_{v_h \in Bh^\perp} b(v_h, q_h) > 0, \forall q_h \in M_h(\Omega) \tag{88}$$

Proof. Let $Phv \in B_h^\perp$ be given. Using the continuous form of the inf − sup condition (34) and (64), (65) from lemma 8, there exists a $c > 0$ and a $\varrho > 0$ such that:

$$\frac{1}{c} ||P_h v||_{V_h^2} \leq \left| |v| \right|_{1,\Omega} \leq \frac{1}{\varrho} sup_{||q_h||=1} b(v, q_h) = \frac{1}{\varrho} sup_{||q_h||=1} b(P_h v, q_h) \tag{89}$$

Thus,

$$sup_{||q_h||=1} b(P_h v, q_h) > \frac{c}{\varrho} ||P_h v||_{V_h^2}, \forall P_h v \in B_h{}^\perp \tag{90}$$

According to (64) and the second condition of (34), this gives

$$sup_{v^h \in B_h{}^{\perp}} b(v_h, q_h) = sup_{v \in B^{\perp}} b(v, q_h) > 0, \forall q_h \in M_h(\Omega) \tag{91}$$

Remark 2. *With a similar demonstration, the bilinear form* b_2 (28) *on* $V_h^2 \times M_h$ *can be used to verify the* $inf - sup$ *condition cited in theorem 9.*

6. Convergence of WEB-Spline

In this section, a proof is offered that the numerical solution $u_h(u_h^1, u_h^2)$ converges to a weak solution $u(u_1, u_2)$ as $h \to 0$. Moreover, the preceding results are extended in a vector field. According to the $inf - sup$ condition theorem (9) this gives

$$\lambda_0 \, || \, u - u_h \, ||_{1,\Omega} \leq b_2(u - u_h, \psi - \psi_h) \tag{92}$$

In addition, according to lemma (8), $b2(u - uh, \psi - \psi h) = b2(Phu - uh, \psi - \psi h)$, although, according to system (27),

$$b_2(P_h u - u_h, \psi - \psi_h) = a(u_h - P_h u, u_h - P_h u) \tag{93}$$

$$= a(u_h - u + u - P_h u, u_h - u + u - P_h u) \tag{94}$$

$$= a(u_h - u, u_h - u) + a(u_h - u, u - P_h u) \tag{95}$$

$$+ a(u - P_h u, u_h - u) + a(u - P_h u, u - P_h u) \tag{96}$$

$$= a(u_h - u, u_h - u) + a(u - P_h u, u - P_h u) \tag{97}$$

$$+ 2a(uh - u, u - Phu). \tag{98}$$

Using the absolute value gives

$$\lambda_0 \, || \, u - u_h \, ||_{1,\Omega} \leq \; |a(u_h - u, u_h - u)| + |a(u - P_h u, u - P_h u)| + 2|a(u_h - u, u - P_h u)| \tag{99}$$

An estimate of the expression $|a(uh - u, uh - u)|$ generates

$$|a(u - P_h u, u - P_h u)| \leq \int_{\Omega} \mu |\nabla(u - P_h u) : \nabla(u - P_h u)| d\Omega + \int_{\Gamma} B^{-1} A(u - P_h u).(u - P_h u) | d\Gamma \tag{100}$$

Using Lemma 5 in paper [21] and Hölder's inequality thus, generates

$$|a(u - P_h u, u - P_h u)| \leq (\mu + |||B^{-1}A|||) \, \|u - P_h u\|_{1,\Omega} \tag{101}$$

According to Jackson's [5] inequality, this generates

$$|a(u - P_h u, u - P_h u)| \leq (\mu + |||B^{-1}A|||)Ch|| u ||_{2,\Omega} \quad (102)$$

with a constant C that is strictly positive and independent of step h and the norm $||.||_{2,\Omega}$ corresponding to Sobolev's space $H^2(\Omega)$.

Estimating the term $|a(u - uh, u - uh)|$ gives

$$|a(u - uh, u - uh)| \leq (\mu + |||B - 1A|||) || u - uh ||1,\Omega \quad (103)$$

Finally, the term $2|a(uh - u, u - Phu)|$ is estimated

$$2|a(uh - u, u - Phu)| \leq 2 \int_\Omega \mu|\nabla(uh - u): \nabla(u - Phu)|d\Omega + \int_\Gamma B^{-1}A(uh - u).(u - Phu)|d\Gamma \quad (104)$$

$$\leq \quad 2(\mu + |||B - 1A|||) || u - Phu ||1,\Omega|| u - uh ||0,\Omega \quad (105)$$

Assuming that

$$\|u - u_h\|_{0,\Omega} \leq c\, inf_{v \in V_h(\Omega)} \|u - v_h\|_{0,\Omega} \quad (106)$$

the space $V_h(\Omega)$ is a finite dimensional subspace of Hilbert space V (Ω), and hence, the infimum is attained. As the infimum is the best approximation of $P_h u$ of u onto $V_h(\Omega)$, this creates:

$$|| u - u_h ||_{0,\Omega} \leq c || u - P_h u ||_{0,\Omega} \quad (107)$$

The inequality in (105) implies that:

$$2|a(u_h - u, u - P_h u)| \leq 2(\mu + |||B^{-1}A|||)c || u - P_h u ||_{1,\Omega}|| u - P_h u ||_{0,\Omega} \quad (108)$$

$$\leq 2(\mu + |||B^{-1} A|||)c || u - Phu^2 ||_{1,\Omega} \quad (109)$$

while Jackson's inequality supports the following estimate, and for step *h* tends to 0:

$$2|a(u_h - u, u - P_h u)| \leq 2(\mu + |||B^{-1}A|||)c \|u - P_h u\|^2_{1,\Omega} \quad (110)$$

$$\leq 2(\mu + |||B^{-1}A|||)c'h\|u\|_{2,\Omega} \quad (111)$$

Using inequalities (102), (103) and (111), gives

$$(\lambda 0 - \mu - |||B-1A|||) || u - uh ||1,\Omega \leq 2(\mu + |||B-1A|||)c' h \ || u ||2,\Omega + (\mu + |||B-1A|||)Ch || u ||2,\Omega \quad (112)$$

allowing the following $H^1(\Omega)$-error estimates for $u - u_h$ to be generated:

$$|| u - u_h ||_{1,\Omega} \leq \beta h \quad (113)$$

This is true as long as $\lambda 0 - \mu - |||B^{-1}A||| > 0$ and β is a positive constant strictly independent of step *h*.

7. Matrix Form of the Navier Lamé Problem

After establishing the discrete inf − sup condition, it is possible to prove both the existence and uniqueness of the discrete solution, common to both the linear-constant and quadratic-linear elements; thus, here, the finite element spaces are labelled V_h and M_h for general application. To find the discrete solution pair $(u_h, \psi_h) \in V_h \times M_h$

It is sufficient to find the coefficient vectors of displacement $u := (u^1, u^2)^T$ where $u^\alpha = (\underset{i}{u}^\alpha)_{i\in I^u})^T$,

$\alpha = 1, 2$ and dilatation $\psi := (\psi_j)_{j\in I^\psi})^T$.

Assuming that:

$$(B^{-1}A)_{\alpha\beta} = \xi_{\alpha\beta} \tag{114}$$

$$(B^{-1})_{\alpha\beta} = \xi_{\alpha\beta}, \forall\alpha, \beta = 1, 2 \tag{115}$$

Then defining:

$$A^\alpha_{i,j} = \int_\Omega \mu\nabla\emptyset_i.\nabla\emptyset_k d\Omega + \int_\Gamma \xi_{\alpha\alpha}\emptyset_i\emptyset_k d\Gamma \tag{116}$$

$$B^\alpha_{i,j} = \int_\Omega (\mu+\lambda)\varphi_j \frac{\partial\phi_i}{\partial x_\alpha} d\Omega \tag{117}$$

$$B^\alpha_{i,j} = \int_\Omega (\mu+\lambda)\varphi_j \frac{\partial\phi_i}{\partial x_\alpha} d\Omega + \int_\Gamma \mu\varphi_j n\emptyset_i d\Gamma \tag{118}$$

$$D_{m,n} = \int_\Omega (\mu+\lambda)\varphi_m\varphi_n d\Omega \tag{119}$$

$$L^1_s = \int_\Omega f_1\phi_s d\Omega + \int_\Gamma (\zeta_{11}+\zeta_{21})g_1\emptyset_s d\Gamma \tag{120}$$

$$L^2_s = \int_\Omega f_2\phi_s d\Omega + \int_\Gamma (\zeta_{22}+\zeta_{12})g_2\emptyset_s d\Gamma \tag{121}$$

Thus, the matrix form of the discrete Navier- Lamé equations can be written as:

$$\begin{pmatrix} A^1 & 0 & B^1_\Gamma \\ 0 & A^2 & B^1_\Gamma \\ B^{1,T} & B^{2,T} & -D \end{pmatrix}\begin{pmatrix} \overline{u^1} \\ \overline{u^2} \\ \bar{\psi} \end{pmatrix} = \begin{pmatrix} L^1 \\ L^2 \\ 0 \end{pmatrix} \tag{122}$$

By defining the assembled matrices $\mathrm{A} = \mathrm{Diag}(\mathrm{A}^1, \mathrm{A}^2)$, $\mathrm{B}_\Gamma = (\mathrm{B}^1{}_\Gamma, \mathrm{B}^2{}_\Gamma)^{\mathrm{T}}$ $\mathrm{B} = (\mathrm{B}^1, \mathrm{B}^2)$, and $\mathrm{F} = (\mathrm{L}^1, \mathrm{L}^2)^{\mathrm{T}}$, the matrix form can be rewritten as:

$$\begin{pmatrix} A & B_\Gamma \\ B^T & -D \end{pmatrix}\begin{pmatrix} \bar{u} \\ \bar{\psi} \end{pmatrix} = \begin{pmatrix} F \\ 0 \end{pmatrix} \tag{123}$$

Theorem 10. The decoupling of dilatation and displacement: Drawing from the matrix form defined above,

$$\begin{cases} A\bar{u} + B_\Gamma\bar{\psi} = F \\ B^T\bar{u} - D\bar{\psi} = 0 \end{cases} \tag{124}$$

Pre-multiplying the first equation by A^{-1} followed by B^{T}, before using the second equation, thus gives:

$$(\mathrm{D} + \mathrm{B}^{\mathrm{T}}\mathrm{A}^{-1}\mathrm{B}_\Gamma)\bar{\psi} = \mathrm{B}^{\mathrm{T}}\mathrm{A}^{-1}\mathrm{F} \tag{125}$$

The following section demonstrates that $\mathrm{D} + \mathrm{B}^{\mathrm{T}}\mathrm{A}^{-1}\mathrm{B}_\Gamma$ is invertible, and that this equation can be solved for $\bar{\psi}$.

Proof. The positive definiteness of this matrix follows from $\mathrm{D} + \mathrm{B}^{\mathrm{T}}\mathrm{A}^{-1}\mathrm{B}_\Gamma$

Defining $B_\Gamma = B + b_\Gamma$, with $\int_\Gamma \mu\varphi_j n\emptyset_i d\Gamma$

$$\langle(\mathrm{D} + \mathrm{B}^{\mathrm{T}}\mathrm{A}^{-1}\mathrm{B}_\Gamma)\psi, \psi\rangle_{\mathbb{R}^M} = \langle D\psi, \psi\rangle_{\mathbb{R}^M} + \langle \mathrm{B}^{\mathrm{T}}\mathrm{A}^{-1}\mathrm{B}_\Gamma\psi, \psi\rangle_{\mathbb{R}^M} \tag{126}$$

$$= \langle D\psi, \psi \rangle_{\mathbb{R}^M} + \langle \mathrm{A}^{-1}(B + \mathrm{b}_\Gamma)\psi, B\psi \rangle_{\mathbb{R}^M} \quad (127)$$

$$= \langle D\psi, \psi \rangle_{\mathbb{R}^M} + \langle \mathrm{A}^{-1}B\psi, B\psi \rangle_{\mathbb{R}^M} + \langle \mathrm{A}^{-1}b_\Gamma, B\psi \rangle_{\mathbb{R}^M} \quad (128)$$

where M is the cardinality of I^{ψ}.

The positive definiteness of $\mathrm{D} + \mathrm{B}^{\mathrm{T}}\mathrm{A}^{-1}\mathrm{B}_\Gamma$ follows from the positive definiteness of matrix A, which in turn is guaranteed by the coercivity condition. The following inequality is therefore an equivalent condition to the inf − sup condition (34):

$$\|\mathrm{B}\psi\| \geq \varrho \, \|\psi\| \quad (129)$$

Indeed, it gives:

$$\langle \mathrm{A}^{-1}B\psi, B\psi \rangle_{\mathbb{R}^M} \geq \beta \left|\left|\beta\psi\right|\right|^2 \geq \beta\varrho^2 ||\psi||^2 \quad (130)$$

and condition (35) thus gives:

$$\langle D\psi, \psi \rangle_{R^M} \geq \varepsilon ||\psi||^2 \quad (131)$$

The Cauchy-Schwarz inequality then gives:

$$\langle A^{-1}b_\Gamma\psi, B\psi \rangle_{\mathbb{R}^M} \geq -\|A^{-1}b_\Gamma\psi\|\|B\psi\| \quad (132)$$

On the other hand,

$$\|A^{-1}b_\Gamma\psi\| = [\sum_{i\in I^u}((A^{-1}b_\Gamma\psi)_i)^2]^{1/2} = (\sum_{i\in I^u}(\sum_{m\in I^\psi}\sum_{k\in I^u}A^{-1}_{ik}b_{km}\psi_{m1})^2)^{1/2} \quad (133)$$

$$\leq \left(\sum_{i\in I^u}\left(cardI^u cardI^\psi max_{k\in I^u} max_{m\in I^\psi}|A^{-1}_{ik}b_{km}|\sum_{m\in I^\psi}\psi_{m1}\right)^2\right)^{1/2} \quad (134)$$

$$\leq \left((card(I^u))\right)^2 card(I^\psi) max_{k,i\in I^u} max_{m\in I^\psi}|A^{-1}_{ik}b_{km})|)^{\frac{1}{2}}\,\|\psi\| \quad (135)$$

By taking $card(I^\psi) = M$, $card(I^u) = N$, $max_{k,i\in I^u} max_{m\in I^\psi}|A^{-1}_{ik}b_{km})| = \alpha$, it can be shown that

$$\langle A^{-1}b_\Gamma\psi, B\psi \rangle_{\mathbb{R}^M} \geq -N(M\alpha)^{1/2}\varrho\|\psi\|^2 \quad (136)$$

and combining, (108), (109), and (114) gives:

$$\langle (D + B^T A^{-1}B_\Gamma)\psi, \psi \rangle_{\mathbb{R}^M} \geq \left(\beta\varrho^2 + \varepsilon - N\varrho(M\alpha)^{1/2}\right)\|\psi\|^2 \quad (137)$$

As soon as $\beta\varrho^2 + \varepsilon - N\varrho(M\alpha)^{\frac{1}{2}} > 0$, this proves the existence of the discrete solution (*uh, ψh*).

8. Numerical results

8.1. Numerical results in 2D

The performance of the WEB-Spline method for Navier - Lamé problem (18) was tested by taking the centrifugal force || f||= r and the domain Ω (see fig. 5) as a rotating steel disc defined by

$$\Omega = \left\{(x,y)/\left(x-\frac{1}{2}\right)^2 + (y-1/2)^2 \le (\tfrac{1}{2})^2\right\} \setminus (x,y)/\left(x-\frac{1}{2}+d\right)^2 + (y-1/2)^2 \le (r)^2 \quad (138)$$

with r = 0.1, d = 0.06 and the edge of Ω consists of two disjoint parts in the form of two circles $\partial\Omega = \Gamma = \Gamma_D \cup \Gamma_N$ such as

$$\Gamma_D = \left\{(x,y)/\left(x-\frac{1}{2}+d\right)^2 + (y-\tfrac{1}{2})^2 - r^2 = 0\right\} \quad (139)$$

$$\Gamma_N = \left\{(x-\tfrac{1}{2})^2 + (y-\tfrac{1}{2})^2 - (1/2)^2 = 0\right\} \quad (140)$$

As in (49), the Dirichlet matrix is A = I_2 on Γ_D, 0_2 on Γ_N and the Neumann matrix is B = I_2 on Γ_N , 0_2 on Γ_D ; the traction force g = (0, 0) on $\partial\Omega$.

In this section we have tested the performance of the Web-Spline method for the Navier-Lamé (18) problem. Then we have compared the results obtained with those of Abaqus software.

We consider the domain Ω is a rotating steel disk (see fig. 5) defined by (138):

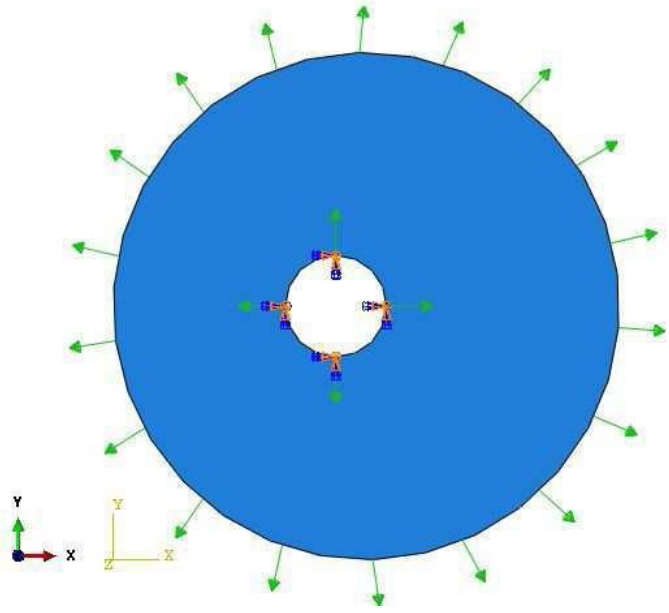

Figure 5: Rotating steel disc

With $r = 0.1$, $d = 0.06$ and the edge of Ω consists of two disjoint parts in the form of two circles.

$$\partial\Omega = \Gamma = \Gamma_D \cup \Gamma_N \quad (141)$$

The centrifugal force was considered as $|| f || = r$.

We assign in (49) to the Dirichlet matrix A = I2 on Γ_D and 0_2 on Γ_N and we give the Neumann matrix: B = I2 on Γ_N, and 0_2 on Γ_D , the tensile force $g = (0, 0)$ on Γ_N .

We refer to the combination of the specific integration rule and the partition of the domain into cells. Numerical integration rules approximate a continuous integral over a domain with a discrete sum:

$$\int f(\xi) d\xi = \sum_{l=1}^{N_q} f(\xi_l)\, w_l$$

where N_q is the number of quadrature points, ξ_l is the coordinate of point l, and w_l is the corresponding weight We restrict this paper to Gaussian quadrature, as it is the most commonly used rule in meshfree methods. The use of Gauss quadrature for arbitrary two-dimensional domains requires the partitioning of the domain into integration cells.

Figures 6 and 9 illustrate the numerical solution of displacement for a steel rotating disk with E = 1, μ = 0.28 fixed on a slightly eccentric axis with radius r. The domain and the direction and size of displacement for each H = (8, 16, 32, 64) cells in each direction are shown. The results are similar to those produced using Abaqus software, suggesting that the web spline approach is sufficiently effective for the resolution of linear elasticity. As noted in the table 1, the precision of numerical approximations was also checked for this example.

To validate the performance of the mixed formulation, we have conducted verification against simulation for the quasi-incompressible material case (E = 1 and u = 0.449). In the end we made a comparison with the commercial software Abaqus as is shown in the figures 10, 11, 12 and 13. The results found show a good agreement with those of Abaqus software.

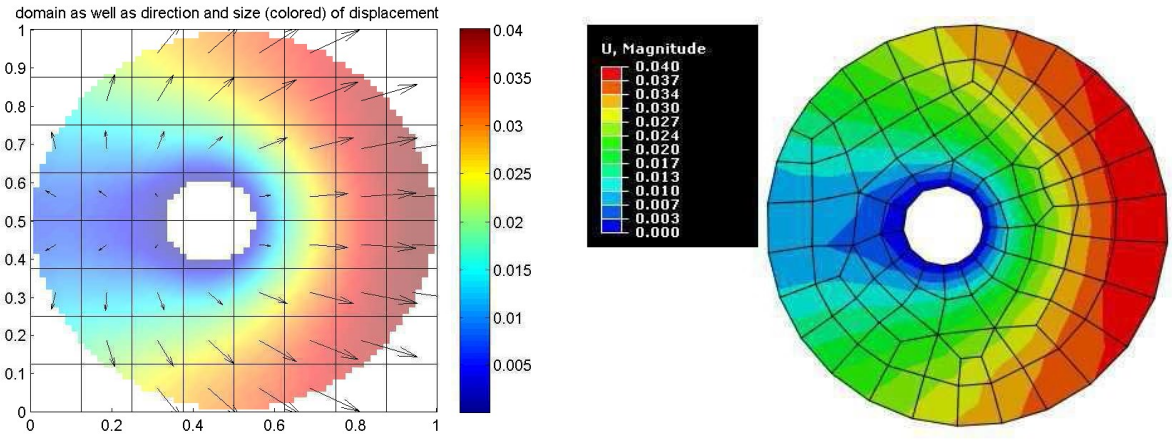

Figure 6: Displacement obtained using the novel method (left), Abaqus (right) for H = 8

As the weighted B-spline basic functions are continuously differentiable for $n \geq 2$ and smooth, the point-by-point residuals for the Navier-Lamé (18) problem can be computed:

$$error\ pde\ = ||\ -\mu\Delta uh\ -\ (\lambda\ +\ \mu)\nabla\psi h\ -\ f\ ||_0 \tag{142}$$

Domain 5 has a smooth edge, and that after a refinement from $H \geq 8$, the error: error pde converges rapidly to 0. For domains with corners, there are resulting singularities. This is due to the fact that the numerical integration used to compute the error integral takes into consideration only the fact that the functions involved are not integrable and the rate.

$$r\ =\ [NaN\ -\ diff\ (log(e))/log(2)] \tag{143}$$

The finite element approximation can be substituted for the partial differential equation in Navier-Lamé where $g = 0$ for a rotating disk. This would not be possible for the standard finite element approximation usually attributed to $H1(\Omega)$. The relative residual for grid widths $1/H = 1/8, \ldots, 1/256$ as thus used, and as the residuals decrease, the rate estimates are seen to show a pattern that increases steadily as H goes from 64 to 256, and the error pde increases from 1,118e+ 000 to 4,462e-004 when H goes from 8 to 256, which can be attributed to numerical stabilities. The main difficulty in solving a linear system is the constraints imposed by non-homogeneous Dirichlet conditions. These constraints create programming difficulties, resulting in the need to apply a Lagrange multiplier method, which in turn generates computational difficulties and enlarges the size of the matrix. This adds to the algorithmic complexity and requires application of iterative methods (Jacobi, Gauss-Seidel, GMRES, etc). The GMRES (Generalized minimal residual) developed by Yousef Saad and Martin H. Schultz in 1986 is a representative example, which gives an approximate solution with a minimal residual; however, this increases the gap between the digital solution and the exact solution.

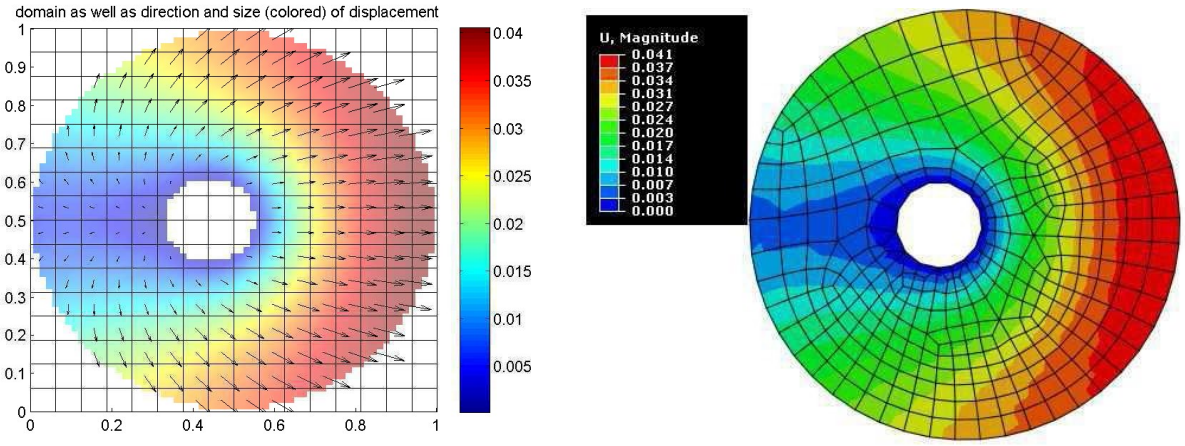

Figure 7: Displacement obtained using the novel method (left), Abaqus (right) for H = 16

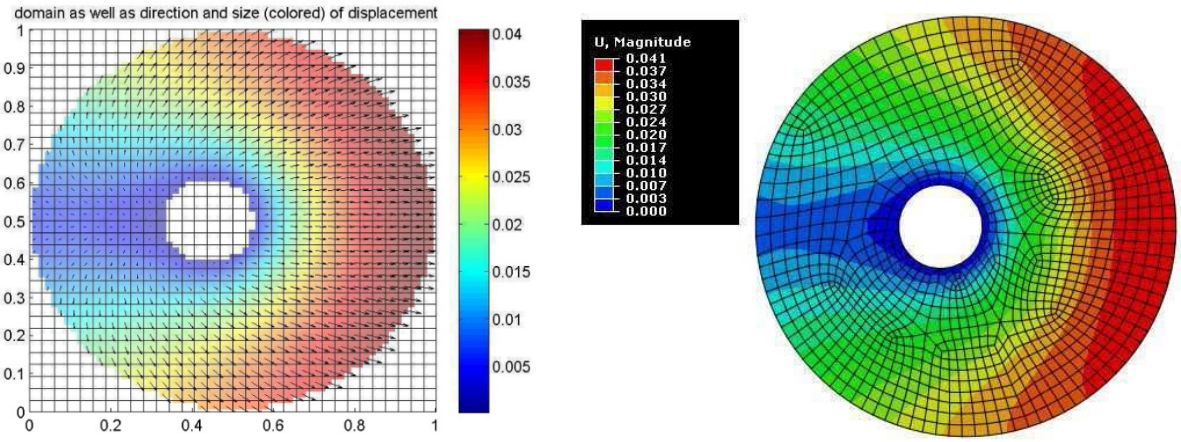

Figure 8: Displacement obtained using the novel method (left), Abaqus (right) for H = 32

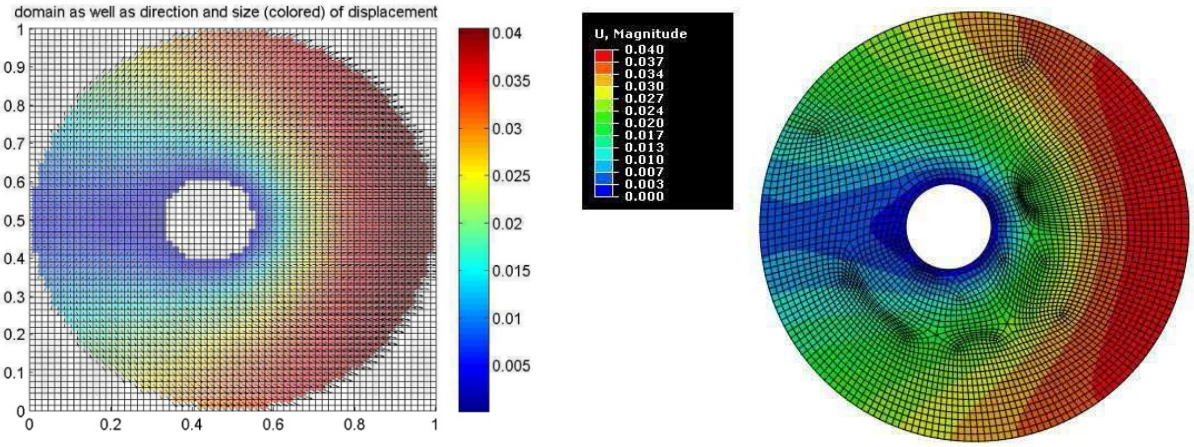

Figure 9: Displacement obtained using the novel method (left), Abaqus (right) for = 64

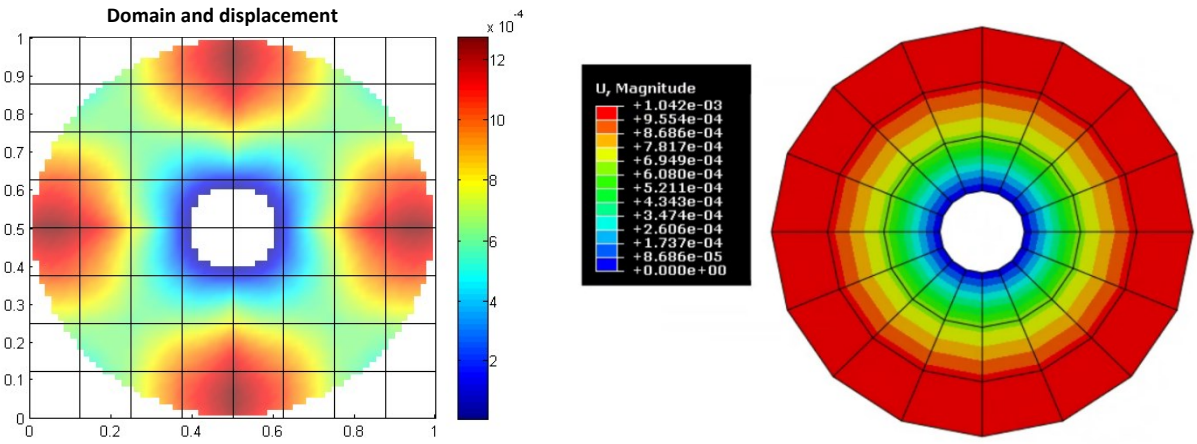

Figure 10: Displacement obtained using the novel method (left), Abaqus (right) for = 8

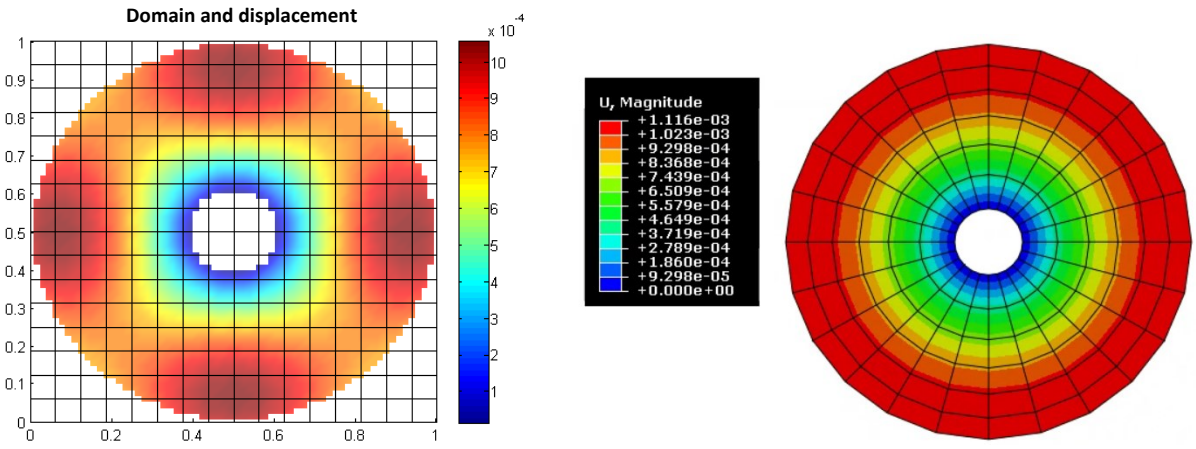

Figure 11: Displacement obtained using the novel method (left), Abaqus (right) for = 16

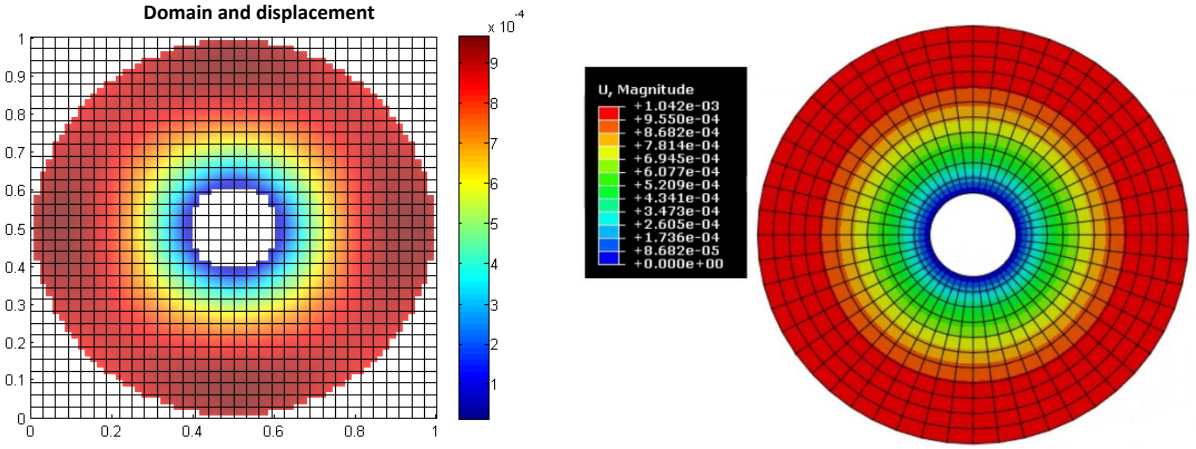

Figure 12: Displacement obtained using the novel method (left), Abaqus (right) for = 32

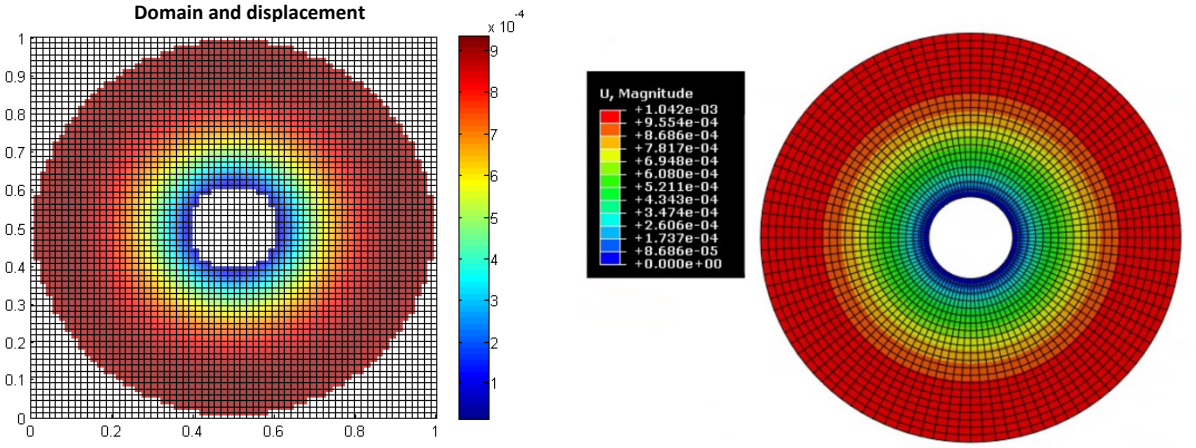

Figure 13: Displacement obtained using the novel method (left), Abaqus (right) for = 64

Table 1: The table showing the different errors

H	Error of PDE	Rate	L2 error	Classical method (Abaqus software)
8	1.118e+000	NaN	3.81647e-002	3.9682e-002
16	3.644e-001	1.618e+000	1.09184e-003	1.1876e-003
32	1.831e-002	4.314e+000	1.13274e-005	1.2151e-005
64	7.003e-003	1.387e+000		
128	1.775e-003	1.980e+000		
256	4.462e-004	1.992e+000		

8.2 Numerical results 3D

An illustration of the feasibility of the 3D Web-spline method is seen in Figure 14, solving the Navier- Lamé system in three dimensions for a concrete dome under gravity.

$$\boldsymbol{f} = -\mu\Delta u - (\lambda + \mu)\nabla(\nabla.u), u = (0,0,0)\ on\ \Gamma \tag{144}$$

According to the physical model (144), with the boundary condition of Dirichlet $u = (0,0,0)$ on Γ,

where u is the displacement, $f\ (f_1, f_2, f_3)$ the body force, Ω the volume occupied by the solid and Γ upper half space. The weight functions can be considered:

$$\omega_\Gamma = 1 - \left(\frac{x-\frac{1}{2}}{R_1}\right)^2 - \left(\frac{y-\frac{1}{2}}{R_2}\right)^2 - \left(\frac{z}{R_3}\right)^2, \omega = -\left(\frac{x-\frac{1}{2}}{r_1}\right)^2 - \left(\frac{y-\frac{1}{2}}{r_2}\right)^2 - \left(\frac{z}{r_3}\right)^2$$

The geometric domain Ω is then represented by the set difference of two sets such as:

$$\Omega = \{(x,y,z) \in [0,1]^3/\omega\Gamma(x,y,z) > 0\}\backslash\{(x,y,z) \in \mathrm{R}_3/\omega(x,y,z) > 0 \tag{145}$$

Similarly, the Γ edge of domain is represented by the following set:

$$\Gamma = \{(x,y,z) \in [0,1]^3/\omega\Gamma(x,y,z) = 0\} \tag{146}$$

Taking $(r_1, r_2, r_3) = (5/20, 5/20, 10/20)$ and $(R_1, R_2, R_3) = (9/20, 9/20, 18/20)$.

The finite element approximation $\omega_\Gamma\ u_h$ has the form:

$$\omega_\Gamma(u_h^1, u_h^2, u_h^3) = \omega_\Gamma \sum_{k\in K}(u_h^1, u_h^2, u_h^3)\, B_k \tag{147}$$

which gives

$$\omega_\Gamma(u_h^1, u_h^2, u_h^3) = \omega_\Gamma \sum_{k\in K}\sum_{i=1}^{3} u_{i,k}\, B_k e_i \tag{148}$$

with e_1, e_2, e_3 as the unit vectors in R^3. By retaining irrelevant B-splines (those with zero coefficients), the index set K becomes a rectangular array.

The cube $[0, 1]^3$ is only the set used to define the B-Spline basis, with the domain for the FEM Simulation being the curved set inside this cube. The B-Splines are thus restricted to this set, and only the part which overlaps the curved set is used.

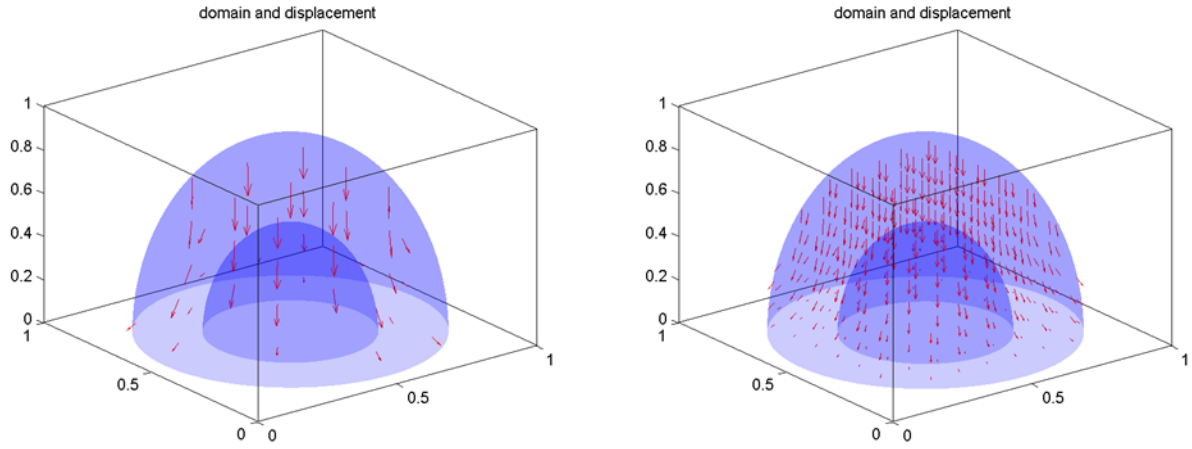

Figure 14: Displacement for a concrete dome under gravity: H=5 (left), for H = 10 (right)

Table 2: The table showing the different data and error of ls and pde

H	Inner cells	Boundary cells	Outer cells	Error of linear system (ls)	Error of PDE
5	1	98	26	1.143e-006	1.584e+000
10	120	428	452	4.484e-009	1.688e+000
15	637	950	1788	3.508e-010	Out of memory

As noted in table 2, the error of pde being greater than 1 is due to lack of regularity in the solution, and thus is not necessarily caused by a bad discretisation.

For larger H, equivalent to smaller grid width, the linear system must be solved more accurately to reduce the finite element error. Ideally, ls = 0, indicating that the system is solved exactly; however, the number of unknowns makes this both not possible and not necessary. The linear system error must, however, be a bit smaller than the finite element error, and the smaller the better.

	Web-Spline (Matlab)	Abaqus Software
Time (s)	19,8521	20,1489

Conclusion

This paper used the equations of linear elasticity to generate a model problem with a novel boundary condition $C_{A,B}$. In order to validate the proposed condition, the proposed weighted B-splines were verified using a mixed finite

element approach as compared to the classical numerical finite element method applied in Abaqus software. The results shown that the WEB-spline based quadratic- linear finite elements satisfy the inf – sup condition necessary for the existence and uniqueness of a solution. This was demonstrated by proving the existence of the discrete solution, and full convergence was established using the numerical solution for the quadratic case. Due to the limited regularity of the Navier-Lamé problem, this is not changed by increasing the degree of the WEB-Spline.

The computed relative errors and their rates indicate that they are of order 1*/H*. Thus, their theoretical validity for numerical solution stability is proved. The advantage of utilising a problem with the $C_{A,B}$ boundary condition was thus shown to be a reduction in MATLAB programming complexity, allowing the development of a single MATLAB file to solve a range of ordinary problems as Dirichlet and Neumann boundaries.

References:

[1] P.Ciarlet,JR.,Jianguo Huang, and Jun zou.some observation ongeneralized saddle-point prob- lem . Society for Industrial and Applied Mathematics Vol.25, No. 1, pp. 224-236. 2003.

[2] O.C. Zienkiewicz and R.I. Taylor, Finite Element Method, Vols. IIII Butterworth and Heine- mann, 2000.

[3] K. Hllig, U. Reif, J. Wipper, Weighted extended B-spline approximation of Dirichlet problems, SIAM J. Numer. Anal. 39 442-462. 2001.

[4] J.A. Cottrell, T.J.R. Hughes, Y. Bazilevs, Isogeometric Analysis: Toward Integration of CAD and FEA, Wiley, 2009.

[5] K. Hllig, Finite Element Methods with B-Splines, SIAM, 2003.

[6] K. Hllig, J. Hrner, A. Hoffacker, Finite element analysis with B-splines: weighted and isogeo- metric methods, in: J.D. Boissonnat, et al. (Eds.), Curves and Surfaces 2011, in: LNCS, vol. 6920, Springer , pp. 330 350. 2012.

[7] Sadd MH. Elasticity: Theory, Application and Numerics. Amsterdam: Elsevier Butterworth Heinemann; 2005.

[8] Timoshenko SP, Goodier JN. Theory of Elasticity. McGraw-Hill; New York: 1985.

[9] K. Atkinson and W. Han . Theoretical Numerical Analysis A Functional Analysis Framework.

TAM 39, Springer, Berlin. 2000.

[10] S. Kesavan . Topics in Functional Analysis and Applications. Wiley Eastern Limited, New Delhi, India. 1989.

[11] K. Hollig, U. Reif, and J. Wipper. Multigrid methods with WEB-splines. NuMat. 912:237 256.

2002.

[12] V. V. K. Srinivas Kumar, B. V. Rathish Kumar, and P. C. Das . WEB-spline based mesh-free fi- nite element analysis for the approximation of the stationary Navier-stokes problem. Nonlinear Anal. 68:3266 3282. 2008.

[13] V. V. K. Srinivas Kumar, B. V. Rathish Kumar, and P. C. Das . A new class of stabilized mesh- free finite elements for the approximation of the Stokes problem. Numer. Meth. Part. D. E. 20:703 722. 2004.

[14] H. J. Choe, D. Kim, H. H. Kim, and Y. Kim. Mesh-less method for the stationary incompress- ible Navier-Stokes equations. Discrete and Continuous Dynamical Systems Series B 1: 495 526. 2001

[15] K. Ho¨llig and J. Ho¨rner, Programming finite element methods with weighted B-splines, Com- puters and Mathematics with Applications 70(7), 1441-1456 (2015).

[16] C. Apprich, K. Hollig, J. Ho¨rner, A. Keller and E. Nava Yazdani, Finite Element Approxima- tion with Hierarchical B-Splines, in Curves and Surfaces 2014, LNCS 9213, 1-15, Springer. 2015.

[17] C. Apprich, K. Hollig, J. Hrner, U. Reif: Collocation with WEB-Splines. Advances in Compu- tational Mathematics (42-4), Springer, 823-842. 2016.

[18] W.H. Zhang, L.Y. Zhao, S.Y. Cai, Shape optimization of Dirichlet boundaries based on weighted B-spline finite cell method and level-set function, Comput. Methods Appl. Mech. Engrg. 294 359 383. 2015.

[19] Weihong Zhang., Linying Zhao, Exact imposition of inhomogeneous Dirichlet boundary con- ditions based on weighted finite cell method and level-set function Comput. Methods Appl. Mech. Engrg. 307 316 338. 2016.

[20] V.L. Rvachev, T.I. Sheiko, V. Shapiro, I. Tsukanov, Transfinite interpolation over implicitly defined sets, Comput. Aided Geom. Design 18 195-220 .2001.

[21] Ouadie Koubaiti, Jaouad El-mekkaoui, and Ahmed Elkhalfi. Complete study for solving Navier-Lame´ equation with new boundary condition using mini element method. INTER- NATIONAL JOURNAL OF MECHANICS, Volume 12, Pages: 46-58. 2018.

[22] Ouadie Koubaiti, Ahmed Elkhalfi, Jaouad El-Mekaoui, Nikos Mastorakis. Solving the problem of constraints due to Dirichlet boundary conditions in the context of the mini element method. INTERNATIONAL JOURNAL OF MECHANICS, Volume 14, Pages: 12-20. 2020.

[23] Ouadie Koubaiti, Jaouad El-mekkaoui, and Ahmed Elkhalfi. ELASTICITY WITH MIXED

FINITE ELEMENT. Communications in Applied Analysis. vol: 22. No: 4. 2018.

[24] Y. Bazilevs, T. J. R. Hughes. NURBS-based isogeometric analysis for the computation of flows about rotating components. Computational Mechanics. Volume 43, Issue 1, pp 143 - 150. De- cember 2008.

[25] JJ Shah, M Ma¨ntyla¨. Parametric and feature-based CAD/CAM: concepts, techniques, and ap- plications. 1995.

[26] H.J. Choe, D.W. Kim, H.H. Kim, Y. Kim Meshless method for the stationary incompressible NavierStokes equations Discrete and Cont. Dynamical Syst. Ser. B, 1 (4) (2001), pp. 495-526.

[27] K. Hollig, U. Reif, J. Wipper Error estimates for the Web-spline method T. Lyche, L.L. Schu- maker (Eds.), Mathematical Methods for Curves and Surfaces, Oslo Vanderbilt University Press, Nashville, TN (2000), pp. 195-209.

[28] K. Hollig, U. Reif, J. Wipper, B-spline Approximation of Neumann Problems, Preprint 2001-2, Universitat Stuttgart.

[29] S. Kesavan Topics in Functional Analysis and Applications Wiley Eastern Limited (1989).

[30] A Özütok, E Madenci. Free vibration analysis of cross-ply laminated composite beams by mixed finite element formulation. International journal of structural stability and dynamics 13 (02), 1250056. 2013.

[31] A Özütok, E Madenci. Static analysis of laminated composite beams based on higher-order shear deformation theory by using mixed-type finite element method. International Journal of Mechanical Sciences 130, 234-243. 2017.

[32] A Özütok, E Madenci, F Kadioglu . Free vibration analysis of angle-ply laminate composite beams by mixed finite element formulation using the Gâteaux differential. Science and Engineering of Composite Materials 21 (2), 257-266. 2014.

[33] E Madenci. A refined functional and mixed formulation to static analyses of fgm beams. Structural Engineering and Mechanics 69 (4), 427-437. 2019.

[34] E Madenci, A Özütok. Variational Approximate and Mixed-Finite Element Solution for Static Analysis of Laminated Composite Plates. Solid State Phenomena 267, 35-39. 2017.

[35] E Madenci, A Özütok. Variational approximate for high order bending analysis of laminated composite plates. Structural Engineering and Mechanics 73 (1), 97. 2020.

[36] H.A.F.A. Santos and J.P. Moitinho de Almeida, A family of Piola-Kirchhoff hybrid stress finite elements for two-dimensional linear elasticity. Finite Elements in Analysis and Design 85 (2014): 33-49.